Understanding adsorption of hydrogen atoms on graphene

Simone Casolo, Ole Martin Løvvik, Rocco Martinazzo, and Gian Franco Tantardini

Citation: The Journal of Chemical Physics **130**, 054704 (2009); doi: 10.1063/1.3072333

View online: http://dx.doi.org/10.1063/1.3072333

View Table of Contents: http://scitation.aip.org/content/aip/journal/jcp/130/5?ver=pdfcov

Published by the AIP Publishing

Understanding adsorption of hydrogen atoms on graphene

Simone Casolo,[1,a)] Ole Martin Løvvik,[1,2] Rocco Martinazzo,[3,b)] and Gian Franco Tantardini[3,4]
[1]*Department of Physics, University of Oslo, P.O. Box 1048 Blindern, NO-0316 Oslo, Norway*
[2]*SINTEF Materials and Chemistry, Forskningsvn 1, NO-0314 Oslo, Norway*
[3]*Department of Physical Chemistry and Electrochemistry and CIMAINA, University of Milan, V. Golgi 19, 20133 Milan, Italy*
[4]*Institute for Molecular Science and Technology (ISTM), V. Golgi 19, 20133 Milan, Italy*

(Received 1 October 2008; accepted 22 December 2008; published online 4 February 2009)

Adsorption of hydrogen atoms on a single graphite sheet (graphene) has been investigated by first-principles electronic structure means, employing plane-wave based periodic density functional theory. A 5×5 surface unit cell has been adopted to study single and multiple adsorptions of H atoms. Binding and barrier energies for sequential sticking have been computed for a number of configurations involving adsorption on top of carbon atoms. We find that binding energies per atom range from ~0.8 to ~1.9 eV, with barriers to sticking in the range 0.0–0.15 eV. In addition, depending on the number and location of adsorbed hydrogen atoms, we find that magnetic structures may form in which spin density localizes on a $\sqrt{3}\times\sqrt{3}R30°$ sublattice and that binding (barrier) energies for sequential adsorption increase (decrease) linearly with the site-integrated magnetization. These results can be rationalized with the help of the valence-bond resonance theory of planar π conjugated systems and suggest that preferential sticking due to barrierless adsorption is limited to formation of hydrogen pairs. © *2009 American Institute of Physics*.
[DOI: 10.1063/1.3072333]

I. INTRODUCTION

Recent years have witnessed an ever growing interest in carbon-based materials. Carbon, being a small atom with a half-filled shell, is able to mix its valence *s* and *p* orbitals to various degrees, thereby forming the building block for extended structures of incredibly different electronic, magnetic, and mechanical properties. Among them, those formed by sp^2 C atoms have attracted much attention in the past few years. They can be collectively termed as graphitic compounds and comprise graphite, carbon nanotubes, fullerenes, polycyclic aromatic hydrocarbons (PAHs), and recently graphene (the one-atom thick layer of graphite) and graphene nanoribbons (GNRs). In particular, the revolutionary (and embarrassing simple) fabrication of graphene[1] has opened the way for a wealth of studies in both fundamental and applied science. New extraordinary properties have become available to material design since its isolation. Indeed, even though they have been known since the first theoretical analysis by Wallace,[2] it was only the experimental observation of the existence of the one-atom thick layer of graphite that triggered much of the current interest. In particular, one of the most interesting aspects of graphene is that it presents low energy excitations as massless, chiral, Dirac fermions mimicking the physics of quantum electrodynamics.[3–5]

In this context, adsorption of hydrogen atoms on graphene and GNRs can be used to tailor electronic and magnetic properties, as already suggested for other "defects," with the advantage of being much easier to realize than, e.g., vacancies. In addition, interaction of hydrogen atoms with graphitic compounds has been playing an important role in a number of fields as diverse as nuclear fusion,[6,7] hydrogen storage,[8] and interstellar chemistry.[9]

In material design for hydrogen storage, several carbon-based structures have been proposed as candidates,[8] in particular, in connection with the spillover effect following embedding of metallic nanoparticles. Though these materials are in practice still far from the wt % target stated by the U.S. Department of Energy, they remain a cheap and safe alternative, and a deeper understanding of the mechanisms underlying adsorption may lead in future to a more efficient material design.

In interstellar chemistry hydrogen-graphite and hydrogen-PAH systems have become realistic models to investigate molecular hydrogen formation in the interstellar medium (ISM). There are still open questions in this context since, in spite of continuous destruction by UV radiation and cosmic rays, H_2 is the most abundant molecule of the ISM. It is now widely accepted that H_2 can only form on the surface of interstellar dust grains and particles,[10–12] which—with the exception of cold dense molecular clouds—are either carbon-coated silicate grains or carbonaceous particles or large PAHs.[13–15] This finding has stimulated a number of theoretical[16–33] and experimental[19,34–43] studies on hydrogen graphitic systems aimed at elucidating the possible reaction pathways leading ultimately to molecule formation.

One interesting finding of these studies is the tendency of hydrogen atoms to cluster at all but very low coverage conditions.[37–39,43] New mechanisms for hydrogen

[a)]On leave from Department of Physical Chemistry and Electrochemistry, University of Milan.
[b)]Electronic mail: rocco.martinazzo@unimi.it.

sticking[25,39] and new recombination pathways[38] have been proposed, based on the now common agreement that the presence of one or more adsorbate atoms strongly influences subsequent adsorption. It is clear that such an influence can only result as a consequence of a substrate-mediated interaction which makes use of the unusual electronic properties of graphitic compounds, but at present a comprehensive model for multiple chemisorptions is still missing.

In this work we present first-principles calculations of single and multiple adsorptions of hydrogen atoms on a graphene sheet, used as a model graphitic material, with the aim of understanding the relationship between the substrate electronic properties and the stability of various cluster configurations. This work parallels analogous investigations of defects in graphene and GNRs.[44–49] Indeed, they all share the disappearance of one or more carbon p orbitals from the π-π^* band system, a fact which may lead to the appearance of magnetic textures and introduce site-specific dependence of the chemical properties. Complementing previous investigations, however, we show how the simple π resonance chemical model helps in rationalizing the findings. A parallel work on different graphitic substrates (PAHs) will follow shortly.[50]

This paper is organized as follows. Details of our first-principles calculations are given in Sec. II, and their results in Sec. III, where we analyze adsorption of a single H atom and briefly introduce the chemical picture (Sec. III A), we consider formation of pairs (Sec. III B) and formation of three- and four-atom clusters (Sec. III C). We summarize and conclude in Sec. IV.

II. COMPUTATIONAL METHOD

Periodic density functional theory (DFT) as implemented in the Vienna *ab initio* simulation package suite (VASP)[51–54] has been used in all the calculations. The projector-augmented wave method within the frozen core approximation has been used to describe the electron-core interaction,[55,56] with a Perdew–Burke–Ernzerhof[57,58] functional within the generalized gradient approximation. Due to the crucial role that spin plays in this system all our calculations have been performed in a spin unrestricted framework.

All calculations have used an energy cutoff of 500 eV and a $6\times6\times1$ Γ-centered **k**-point mesh to span the electron density, in a way to include all the special points of the cell. The linear tetrahedron method with Blöchl corrections is used.[59] All the atomic positions have been fully relaxed until the Hellmann–Feynman forces dropped below 10^{-2} eV Å^{-1}, while convergence of the electronic structures has been ensured by forcing the energy difference in the self-consistent cycle to be below 10^{-6} eV. In order to compute energy barriers partial occupancy of one-particle states has been allowed with a 0.05 eV wide Gaussian smearing, and electronic solutions have been carefully checked to represent the correct spin-polarized ones needed to describe bond-breaking/bond-forming processes.

The slab supercell considered has been carefully tested and a 20 Å vacuum along the c axis has been adopted to ensure no reciprocal interaction between periodic images.

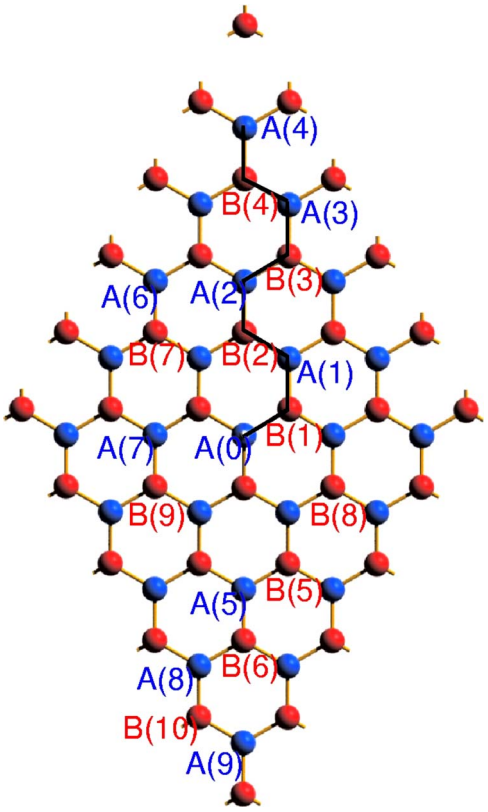

FIG. 1. (Color online) The graphene unit cell used for the calculations with A (blue) and B (red) lattice sites indicated. Also indicated is the path used for Fig. 3, $A(0)$ being the first H adsorption site.

We find that by using the above settings the interaction between two adjacent graphite layers is ~2 meV, largely within the intrinsic DFT error. This result is in agreement with literature data.[60,61] For this reason a single graphene sheet can also model the Bernal (0001) graphite surface, at least as long as chemical interactions are of concern.

The cell size on the surface plane is a fundamental parameter for these calculations since we have found that chemisorption energies strongly depend on the coverage (see below). We choose to use a relatively large 5×5 cell in order to get some tens of meV accuracy while keeping the computational cost as low as possible. Even with this size, however, the possibility of interactions between images has always to be taken into account when rationalizing the data.

The cell used in this work is shown in Fig. 1, along with a labeling system for a number of lattice sites. Note that the graphene lattice consists of two equivalent sublattices (here and in the following denoted as A and B) which may become no longer equivalent upon H adsorption.

III. RESULTS

A. Single atom adsorption

Chemisorption of single H atoms on graphite has long been studied since the works of Jeloaica and Sidis[16] and Sha and Jackson,[17] who first predicted surface reconstruction upon sticking. Such a reconstruction, i.e., the puckering of the carbon atom beneath the adsorbed hydrogen atom, occurs as a consequence of sp^2–sp^3 rehybridization of the valence

TABLE I. Chemisorption energy (E_{chem}) and equilibrium height of the C atom above the surface (d_{puck}) for H adsorption on top of a C atom, for a number of surface unit cells, corresponding to different coverages θ.

Unit cell	θ (ML)	d_{puck} (Å) This work	d_{puck} (Å) Others	E_{chem} (eV) This work	E_{chem} (eV) Others
2×2	0.125	0.36	0.36[a]	0.75	0.67[a]
3×3	0.062	0.42	0.41[b]	0.77	0.76[b]
Cluster	0.045	⋯	0.57[c]	⋯	0.76[c]
4×4	0.031	0.48	⋯	0.79	0.76,[d] 0.85[e]
5×5	0.020	0.59	⋯	0.84	0.71,[f] 0.82[g]
8×8	0.008	⋯	⋯	⋯	0.87[h]

[a]Reference 17.
[b]Reference 62.
[c]Reference 63.
[d]Reference 64.
[e]Reference 39.
[f]Reference 65.
[g]Reference 66.
[h]Reference 67.

C orbitals needed to form the σ CH bond. Since this electronic/nuclear rearrangement causes the appearance of an energy barrier ~0.2 eV high, sticking of hydrogen atoms turns out to be a thermally activated process which hardly occurs at and below room temperature.[62]

As already said in Sec. II, we have reconsidered adsorption of single hydrogen atoms for different sizes of the surface unit cell. We have found that both the binding energy and the puckering height are strongly affected by the size of the unit cell (see Table I), and even the results of the 5×5 cell turn out to be in error of about ~30 meV with respect to the isolated atom limit estimated by the calculation at 0.008 ML coverage.[67] In particular, we have found that some caution is needed when comparing the height of the carbon atom involved in the bond since constraining the neighboring carbon atoms in geometry optimization may lead to considerable surface strain.

Despite this, we have consistently used the 5×5 cell in studying multiple adsorptions of hydrogen atoms. Indeed, this size allowed us to investigate a number of stable configurations involving two, three, and four adsorbed H atoms, along with the barrier to their formation, with the same setup described in Sec. II. Interactions between images do indeed occur for some configurations but, as we show below, this does not prevent us to get a clear picture of the adsorption processes we are interested in.

In agreement with previous studies we find that hydrogen adsorption can only occur if the substrate is allowed to relax. Without relaxation the adsorption curves on different surface sites are repulsive, and only a metastable minimum is found for the atop position.[17] Surface relaxation requires about 0.8–0.9 eV (this is the energy needed to pucker the free graphene sheet as required by adsorbing one H atom on top of a carbon atom) and results in the outward motion of the carbon atom forming the CH bond (see Table I and Refs. 16 and 17). We note that the results of Boukhvalov *et al.*[68] are at variance with a number of literature data (see, e.g., Table I and reference therein, compared with Table I of Ref. 68). Special care was therefore devoted to try to reproduce their energetic and geometrical results, without any success. We carefully checked our convergence of electronic and geometrical optimizations, and Sec. II should give enough details to guarantee data reproducibility.

In addition, we have investigated the electronic substrate properties of the resulting hydrogenated graphene, in order to get hints for understanding the adsorption process of additional atoms. In Fig. 2 we show the density of states (DOS) of the 5×5 H-graphene equilibrium structure (bottom panel), compared to that of clean graphene (top panel). It is evident from the figure that hydrogen adsorption causes the appearance of a double peak in the DOS, symmetrically placed around the Fermi level. This is in agreement with rigorous results that can be obtained in tight-binding theory for *bipartite* lattices. Indeed, Inui *et al.*[69] showed that for a bipartite lattice with n_A A lattice sites and n_B B lattice sites a sufficient condition for the existence of midgap states is a lattice imbalance ($n_A \neq n_B$). In particular, there exist $n_I=|n_A-n_B|$ midgap states with *vanishing* wavefunction on the minority lattice sites. In H-graphene a lattice imbalance results

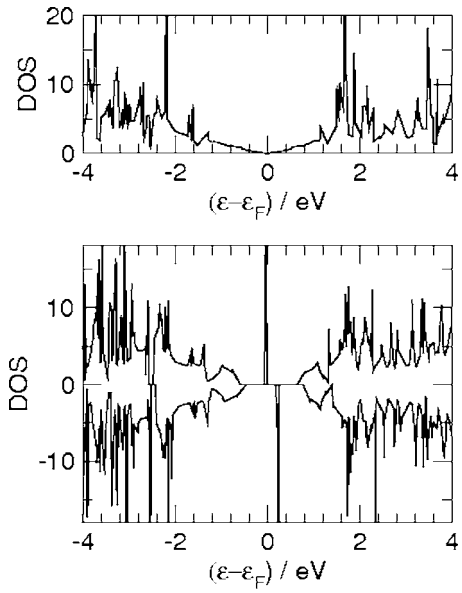

FIG. 2. Top panel: Total DOS for graphene. Bottom panel: DOS for spin-up (positive values) and spin-down (negative values) components in a 5×5 H layer on graphene.

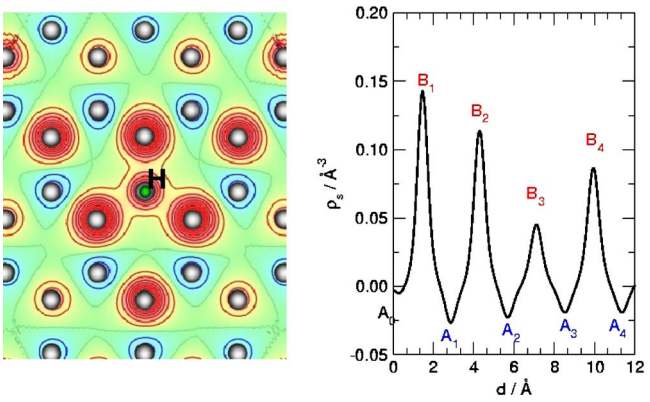

FIG. 3. (Color online) Spin density at 0.47 Å above the graphene surface after adsorption of a hydrogen atom. Left: Contour map with red/blue lines for spin-up/spin-down excess, respectively. Right: Spin density at the same height as on the left panel, along a path joining the C atoms (for the labels see Fig. 1).

as a consequence of the bond with the H atom which makes one of the p orbitals no longer available for taking part to the π-π^* band system. There is one midgap state for each spin species, and the degeneracy is lifted if exchange-correlation effects are taken into account, as shown in Fig. 2 for our DFT results. This state has been mapped out in Fig. 3 (left panel), where we report a contour map of the spin density at a constant height of 0.47 Å above the surface. It is clear from the figure that if adsorption occurs on an A lattice site the spin density (due mainly to the above midgap state) localizes on B lattice sites. The latter now contain most of the $1\mu_B$ magnetization (μ_B denotes Bohr magneton) previously carried by the H atom species, and a slight spin-down excess on A sites results as a consequence of the spin polarization of the lower-lying states. This is made clearer in the right panel of Fig. 3 where we report the spin density at the same height above the surface as before along a rectilinear path joining a number of C atom sites away from the adsorption site (see Fig. 1 for the labels). Note that the spin density decays only slowly with the distance from the adsorption site, in agreement with theoretical results that suggest that in the case of two dimensional graphene this decay corresponds to a non-normalizable state with a $1/r$ tail (in contrast to nonzero gap substrates such as armchair nanoribbons where midgap states are normalizable).[44] With our unit cell the effect of the interaction with the images is already evident at rather short distances, but as we show below, this effect has no influence on the interpretation of the results. Note also that this spin pattern is common to other defects (e.g., vacancies, voids, and edges) which have been known for some time to strongly modify the electronic properties of graphene and graphene-like structures and to (possibly) produce long-range ordered magnetic structures.[44–49,67,70–75] In particular, in a recent comprehensive study Palacios *et al.*,[48] using a mean-field Hubbard model for graphene, clarified the appearance of magnetic textures associated with vacancies and predicted the emergence of magnetic order. Their model also suits well to defects such as the presence of adsorbed hydrogen atoms.

From a chemical point of view the above spin pattern (and the resulting magnetic properties) arises from the well-known "spin alternation" typical of π conjugated compounds. This behavior is easily understood in terms of resonant chemical structures, such as those shown in Fig. 4 for a coronene molecule. In this and analogous PAHs, the π electron system can be described as a combination of conventional alternated double bond structures, like the ones shown in Fig. 4 (see a). Once a hydrogen atom has been adsorbed on the surface, an unpaired electron is left on one of the neighboring C atoms (b, left panel), which can subsequently move in each of the carbon atoms belonging to a sublattice $\sqrt{3}\times\sqrt{3}R30°$ by "bond switching" (see b and c). Spin alternation arises from the "resonant" behavior of an unpaired electron in α position (the nearest neighbor one) with respect to a double bond: such "resonance" can be naively viewed as the spin recoupling of the unpaired electron with the electron on the neighboring site, a process which sets free a second electron on the same sublattice.

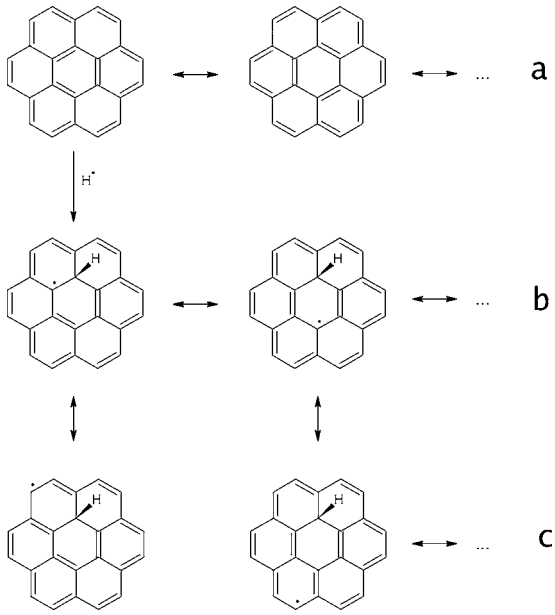

FIG. 4. (a) The π resonating chemical model for a graphenic surrogate (coronene). [(b) and (c)] Spin alternation after hydrogen adsorption.

It is worth noticing at this point that this simple picture has solid roots in quantum mechanics, namely, in the valence bond (VB) theory of chemical bonding.[76] This theory was formulated soon after the advent of quantum mechanics by Heitler and London[77] and Pauling and Slater, and initially aimed at rationalizing successful prequantum ideas about bonding in molecules, such as the Lewis structures and the octet rule. Since the beginning, it correctly described bond-forming and bond-breaking processes and spin-recoupling and hybridization phenomena and provided rigorous justification of concepts such as structures and resonance between structures. Later, it developed as an *ab initio* approach,[78,79] complementary to molecular orbital (MO) based electronic structure theories, with the disadvantage of using nonorthogonal many-electron basis but the advantage of providing a clear picture of electronic structures.

For a π electron system, a simple (correlated) VB *ansatz* for the N electron wavefunction of the π cloud reads as

$$\Psi_{SN} = \mathcal{A}(\phi_1 \phi_2 \cdots \phi_N \Theta_{SN}), \quad (1)$$

where $\mathcal{A}$ is the antisymmetric projector, $\phi_i = \phi_i(\boldsymbol{r})$ for $i = 1, N$ are (spatial) orbitals accommodating the N electrons, and Θ_{SN} is an N electron spin function with spin quantum number S. The latter is usually variationally optimized by expansion on a spin basis $\{\Theta_{SN;k}\}_{k=1,f_S^N}$ of $\mathbf{S}^2$ eigenvectors with eigenvalue $S(S+1)$ (and given magnetization). Chemical ideas are brought into the theory by using the "perfect pairing" spin basis devised by Rumer[80] in which, for a given S and $M_s = S$, the total magnetization is given by $2S$ electrons coupled at high spin, the remaining $N-2S$ being accommodated in $(N-2S)/2$ singlet-coupled pairs. Indeed, if the orbitals ϕ_i are *localized* on the atoms, the resulting wavefunction

$$\Psi_{SN} = \sum_{k=1,f_S^N} c_k \mathcal{A}(\phi_1 \phi_2 \cdots \phi_N \Theta_{SN;k}) = \sum_{k=1,f_S^N} c_k \Psi_{SN;k}$$

is a superposition of conventional "structures" $\Psi_{SN;k}$ describing pairs of atom-centered singlet-coupled orbitals (i.e., Lewis chemical bonds and lone pairs) and unpaired electrons. Simple molecules require just one perfect-pairing spin function coupling those pairs of orbitals with substantial overlap. Less conventional molecules, such as π conjugated systems, need a true superposition of two or more spin structures since the energy gain (the *resonance* energy) in allowing such superposition is sizable in these cases. Correspondingly, the classical Lewis picture of chemical bonds is extended to account for the resonance phenomenon, as shown in Fig. 4 with double ended arrows indicating *superposition* of chemical structures.

Early applications of the VB theory used frozen atomic orbitals, whereas nowadays[81–84] both the spin-coupling coefficients c_k and the orbitals can be variationally optimized, even when using a number of configurations in place of the single-orbital product appearing in Eq. (1). The interesting thing is that these optimized orbitals, as a consequence of electron correlation, are usually (if not always) localized on atomic centers and are only slightly polarized by the environment, thereby supporting the interpretation of the simple wavefunction of Eq. (1) as a quantum-mechanical translation of Lewis theory of chemical bond. This is true, in particular, for the benzene molecule, the prototypical π resonant system, where six p-like orbitals are mostly coupled by two so-called Kekulè structures.[85–87] (For $S=0$ and $N=6$ the set of five linearly independent Rumer structures of the benzene π system is given by two Kekulè structures and the three additional "Dewar" structures. With orbital optimization, a resonance energy $\simeq 0.8$ eV can be computed when using two Kekulè structures in place of one, whereas only some tenths of meV are additionally gained when full optimization of the spin function is performed.[50])

From a physical point of view, wavefunction (1) can be considered a generalization to N electron systems of the Heitler–London ansatz forming the basis for the Heisenberg model of magnetism in insulators. In addition, if the orbitals are allowed to be "polarized," bandlike behavior can be accommodated along with collective spin excitations, as in the Hubbard model[88] which has been finding widespread use in investigating graphitic compounds. The fact that Hubbard model, and its Heisenberg limit, can be derived by suitable approximations to VB ansatz has long been known in the chemical literature, especially in connection to π resonant systems (see, e.g., Refs. 89 and 90 and references therein. Hubbard model is also known as Pariser–Parr–Pople model, after Pariser and Parr[91,92] and after Pople[93]). We can roughly say that Heisenberg models correspond to the "classical" valence theory using orbitals constrained to have their free-atom form, whereas Hubbard models arise by allowing them to be deformed by the chemical environment.

In Secs. III B and III C, we will use wavefunction of Eq. (1) as a simple guide to interpret the results of our first-principles calculations, keeping in mind its connections with the traditional chemical picture on the one hand and the Hubbard model on the other hand. As we will show in the following, even at this qualitative level, a number of useful insights can be gained from such a picture.

It is worth noticing at this point that these "VB considerations" do not rely on the existence of any symmetry in the system and therefore apply equally well to symmetric and nonsymmetric systems (like the defective structures considered in Secs. III B and III C or finite-size systems such as PAHs). Symmetry, if present, is best exploited in single-particle theories when single-particle states are eigenfunctions of symmetric effective one-particle Hamiltonians, and indeed notable work has been done on graphene and GNRs with tight-binding Hamiltonians (see, e.g., Ref. 94 for a comprehensive overview). [Note that in the ansatz of Eq. (1)—which has its origin in the separated atom limit—spatial symmetry is inextricably linked to spin space.] Even in these cases, however, correct description of magnetic ordering and related effects on band structures (see, e.g., Ref. 95) needs many-particle theories. The same is true for the bond-breaking/bond-forming processes considered here which, strictly speaking, cannot be handled with single-particle theories because of the well-known static correlation problem.

As a first example we can reconsider adsorption of a single hydrogen atom on graphene. In a diabatic picture (i.e., when constraining the spin coupling to the Kekulé structures of Fig. 4, panel a) the interaction between graphene and the incoming H atom is expected to be repulsive since no electron is available to form the CH bond. On the other hand, a low-lying spin-excited state corresponding to a Dewar-like structure (which has two singlet-paired electrons on opposite, no-overlapping end of a benzene ring) would give rise to an attractive barrierless interaction. At short range, then, an avoided crossing between the two doublet curves occurs which signals the spin transition leading to bond formation, even though this can lead only to a metastable state if surface reconstruction is not allowed, as indeed found in DFT calculations (e.g., see Fig. 2 in Ref. 17). Actually, in this case the situation is a bit more complicated since a slightly lower-lying state in the triplet manifold (obtained by spin flipping the above spin-excited Dewar-like structure) contributes to the same doublet manifold. VB calculations on the simpler H-benzene system confirm this picture,[50] see Fig. 5. [Single-point VB calculations have been performed with the help of

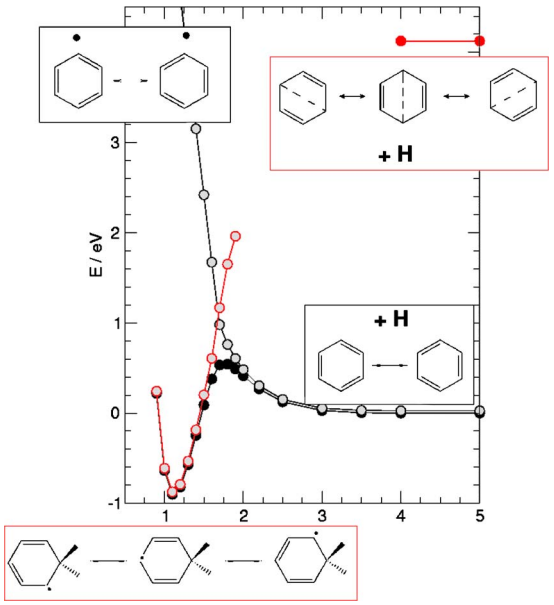

FIG. 5. (Color online) Interpretation of the sticking barrier as an avoided crossing between chemical structures. VB results for the benzene-H system, from Ref. 50. Solid black and red circles for the ground $[C_6H_6(^1A_{1g})+H(^2S)]$ and the first excited states $[C_6H_6(^3B_{1u})+H(^2S)]$, as obtained at the single-orbital-string level of Eq. (1), with orbital optimization. Quasidiabatic results are obtained by properly constraining the spin space. Kelulè structures only (lower right and upper left insets) for empty black circles; structures in the lower left inset for empty red circles. Also shown in the upper right inset are the main (Dewar-like) structures needed to described the $^3B_{1u}$ state of benzene.

the VB2000 code[96,84] on the geometries optimized at the DFT-UB3LYP level, as implemented in the GAMESS code,[97] using in both cases the cc-pVDZ atom-centered basis set. Two group functions[98] have been defined and simultaneously optimized: a VB group containing nine electrons in nine orbitals [Eq. (1)] and a Hartree–Fock (HF) group accommodating the remaining e^- in doubly occupied orbitals. VB orbitals describe the six π electrons of benzene, the electron of the incoming H atom, and the two σ electrons of the CH bond which is most distorted upon adsorption. Standard localization schemes have been employed to obtain the proper guess from HF orbitals. Wavefunction optimizations have been performed in the full spin space for nine electrons in a doublet state, whereas "diabatic" calculations have used the above optimized VB orbitals and constrained spin functions. See Ref. 50 for more details.]

B. Secondary adsorption

Next we consider adsorption of a second atom on the different sites $A(n)$ $(n=1,6)$ and $B(n)$ $(n=1,6)$ shown in Fig. 1, with a first adsorbed H atom on site $A(0)$. For each site we have investigated the ground spin manifold by allowing full relaxation of the magnetization. In addition, in most of the cases, we have also performed magnetization-constrained calculations in order to get insights on both the singlet and the triplet states arising from the interaction between the doublet H-graphene ground-state and the second H atom.

The results for the binding energies are reported in Table II, along with the site-integrated magnetizations (M_{SI}) and the total magnetization M. Site-integrated spin densities have been obtained by integrating the spin density on a small cylinder (of radius half of the C–C distance in the lattice) centered on each site and can be considered a rough measure of the total spin excess available on the site. This quantity behaves very similar to the spin density itself, decreasing in magnitude when increasing the distance from the adsorption site, *separately* for each sublattice. Some exceptions are worth noticing, namely, the $A(0)-B(4)$ pair, and are due to the cumulative effect of next-neighbor images. Notice, however, that despite their possible artificial nature, results corresponding to any lattice sites when viewed *as a function* of the site-integrated magnetization give insights into the adsorption process.

TABLE II. Binding energies (E_{bind}) for secondary adsorption to form the H pairs shown in Fig. 1, along with the site-integrated magnetizations (M_{SI}) before adsorption and the total ground-state magnetization (M) after adsorption obtained when fully relaxing the magnetization. Also reported are the binding energies obtained when the magnetization is constrained to $M=0,2\mu_B$ for A and B sites, respectively. See text for details.

Position	M_{SI} (μ_B)	E_{bind} (eV)	M (μ_B)	E^*_{bind} (eV)
$B(1)$	0.109	1.934	0	0.933
$A(1)$	−0.019	0.802	2	0.575
$B(2)$	0.085	1.894	0	0.828
$A(2)$	−0.017	0.749	2	0.531
$B(3)$	0.040	1.338	0	0.646
$A(3)$	−0.016	0.747	2	0.570
$B(4)$	0.076	1.674	0	⋯
$A(4)$	−0.016	0.747	2	0.573
$B(5)$	0.023	1.033	0	0.590
$A(5)$	−0.014	0.749	2	0.531
$B(6)$	0.028	1.110	0	0.545
$A(6)$	−0.015	0.787	2	⋯

A quick look at Table II reveals that the two sublattices A and B behave very different from each other, as the spin-coupling picture of Fig. 4 (panels b and c) suggests. Roughly speaking, adsorption on the B lattice is *preferred* over that on the A lattice. The binding energies are much larger than the first adsorption energy reported in Table I (they can be as large as twice the adsorption of the first atom) and give rise to a final unmagnetized state. In contrast, the binding energy for adsorption on the A lattice site is comparable to that of single H adsorption, and the ground state of the H pair on graphene is a triplet $(M=2\mu_B)$.

These findings agree with Lieb's theorem[99] for the repulsive Hubbard model of a bipartite lattice and a half-filled band, which states that the ground state of the system has $S=1/2|n_A-n_B|$. In such model, the electronic state of the system would be described by $N-2$ p orbitals (N being the original number of sites), and $n_B=n_A=N/2-1$ if adsorption of the second hydrogen atom proceeds on the B lattice (to form what we can call AB dimers), whereas $n_B=n_A+2=N/2$ if it proceeds on the A lattice (to form A_2 dimers). The results are also consistent with the VB framework sketched in Sec. III A: with reference to Fig. 4 (panels b and c), it is clear that when a H atom adsorbs on a B site its electron readily couples with the unpaired electron available on the B sublattice, whereas when adsorption occurs on an A site *two*

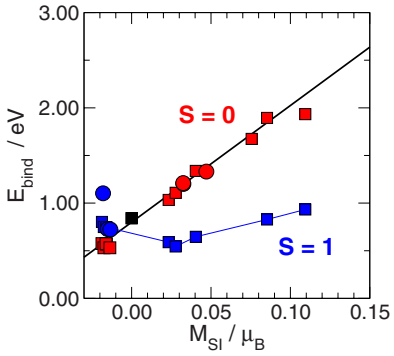

FIG. 6. (Color online) Binding energies for secondary H adsorption as a function of the site-integrated magnetization for singlet (red squares) and triplet (blue squares) states. Black square is the data point for single H adsorption. Also shown is a linear fit to the data set (solid line) and the H binding energy to form some four-atom clusters from three-atom ones (red and blue circles for final singlet and triplet states, respectively). See text for details.

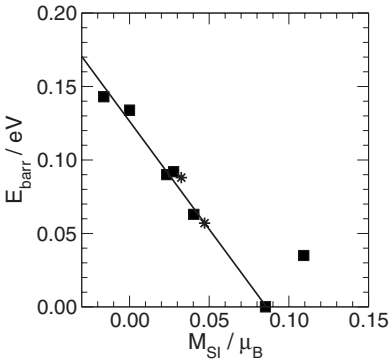

FIG. 7. Barrier energies for secondary atom adsorption as a function of the site-integrated magnetization. Linear regression (solid line) includes all data represented with squares, with the exception of the value of the *ortho* dimer (rightmost point in the graph). Data point at $M_{SI}=0$ is for single H adsorption; star is for forming a four-atom cluster from a three-atom one.

electrons are left in excess on the B sublattice, and they more favorably couple at high spin.

The relationship between the available unpaired electron density at a given site and the binding energy of adsorbing a second H atom can be made clearer by reporting the energy data of Table II as a function of M_{SI}. This is shown in Fig. 6, for both the singlet and triplet states of the dimers, along with the value for the first H adsorption (data point at $M_{SI}=0$). It is clear from the figure that with the exception of the value for the ortho dimer $[A(0)B(1)$ in Fig. 1, this value has been excluded from the linear regression shown in Fig. 6], a linear relationship between the binding energy and the site-integrated magnetization well describes the situation, and the binding energy for single H adsorption fits well to this picture.

This is again consistent with the chemical model, as long as the site-integrated magnetization is a measure of the unpaired electron density available. According to Sec. III A, adsorption of the first hydrogen atom arises from the energy balance between a "localization energy" (the spin excitation needed to set free an unpaired electron on the given lattice site), the spin pairing forming the bond, and the surface reconstruction energy. The same is true for adsorption of a second atom: localization energy takes only a slightly different form than before because an unpaired electron is already available in one of the two sublattices, but surface reconstruction energy is not expected to depend on the adsorption site. [In terms of the wavefunction of Eq. (1) this localization energy can be defined by observing that the structures in which the spin-up density localizes on the $(N-1)$th site (N even) correspond to $\Psi=A(\phi_1\phi_2\cdots\phi_{N-1}\Theta_{\mathrm{loc}}^{N-1})$, where $\Theta_{\mathrm{loc}}^{N-1}$ is constrained to have the form $\Theta_{\mathrm{loc}}^{N-1}=\Theta_{0,0}^{N-2}\alpha$, whereas the ground-state spin function comprises additional contributions from $\Theta_{1,1}^{N-2}\beta$ structures.] Then, adsorption energies depend on the electronic properties only, and the linear behavior observed for singlet-state dimers in Fig. 6 suggests that the energy needed to localize the unpaired electron on a given site decreases *linearly* when increasing the unpaired electron density available. Notice that negative values of M_{SI} (as found at A sites) correspond to a spin excess *parallel* to that of the incoming H electron, and for these sites localization of an unpaired electron with an *antiparallel* spin requires increasingly more energy when the (magnitude of the) spin density increases since this can only be achieved by adding one electron to the site. On the other hand, when a triplet dimer is formed upon adsorption the H electron does not make use of the unpaired electron available, and adsorption energies are all around ~0.8 eV, i.e., of the order of the first H adsorption. The effect of surface relaxation is only seen in forming the ortho dimer, where few tenths of eV more than the single H relaxation energy are required because of the closeness of the two hydrogen atoms.

Analogous linear behavior can be found when considering the computed energy barrier to sticking as a function of the site-integrated magnetization, as shown in Fig. 7 for a number of dimers (in their ground electronic state). This agrees with the above localization energy and with the common tendency for a linear relationship between the binding and the barrier energies for activated chemical reactions (Brønsted–Evans–Polayni rule), the only exception being the ortho dimer considered above. In agreement to previous theoretical studies we find that the para dimer $[A(0)B(2)]$ shows no barrier to adsorption, thereby supporting a preferential sticking mechanism. This mechanism was first suggested by Hornekær *et al.*[39] who looked at the scanning tunneling microscopy images formed by exposing highly oriented pyrolitic graphite samples to a high-energy (1600–2000 K) H atom beam and observed formation of stable pairs, confirmed by first-principles calculations.[25,39]

We therefore find that formation of AB dimers is both thermodynamically and kinetically favored over formation of A_2 dimers and single atom adsorption. This agrees with current experimental observations which show evidence for clustering of hydrogen atoms at all but very low ($<1\%$) coverage conditions. In addition, we notice that the dimers identified so far[37–39] are all of the AB type.

C. Further adsorptions

We consider in this section results concerning formation of clusters of three and four atoms. In these cases, the number of possible configurations is quite large and therefore we

TABLE III. Binding energies (E_{bind}) for addition of a third H atom to the *para* dimer structure $A(0)B(2)$ on the sites indicated in the first column (labels from Fig. 1).

Position	E_{bind} (eV)
$A(2)$	1.516
$B(3)$	0.847
$A(3)$	0.727
$B(4)$ ($\equiv A(5)$)	0.971
$A(4)$ ($\equiv B(6)$)	0.821
$B(7)$	0.727
$B(8)$	1.301

TABLE IV. Binding (E_{bind}) energies for adsorption to form H quadruples from the $A(0)B(2)B(8)$ cluster, along with the site-integrated magnetizations (M_{SI}) and the total ground-state magnetization (M), before and after adsorption, respectively. See Fig. 1 for atom labels.

	M_{SI} (μ_B)	E_{bind} (eV)	M (μ_B)
$B(9)$	−0.0180	1.103	2
$A(7)$	0.0471	1.331	0
$B(6)$	−0.0151	0.727	2
$A(8)$	0.0325	1.210	0
$B(10)$	−0.0134	0.723	2
$A(9)$	0.0326	1.201	0

limit our analysis to a few important cases. Following analogous notation recently introduced for defects by Palacios *et al.*,[48] we use the "chemical formula" A_nB_m to denote a cluster with n H atoms in the A lattice and m H atoms in the B lattice. According to Lieb's theorem and to the π resonance picture, we expect that the ground electronic state has $|n-m|$ unpaired electrons. We have considered a number of A_2B_2, A_2B, A_3B_1, and A_3 clusters and found that their ground state has 0, 1, 2, and $3\mu_B$ of magnetization, respectively, in agreement with the expectation.

Three atom clusters have been obtained by adding one hydrogen atom either to a para dimer or to a meta dimer, i.e., $A(0)B(2)$ and $A(0)A(1)$ with the labels of Fig. 1, respectively. The binding energies of a third hydrogen atom to a para dimer structure are reported in Table III. Since they all are of A_2B type, the total magnetization for the resulting structures is $1\mu_B$. A look at Table III reveals that adsorption to a third hydrogen atom parallels that of the first H. This is consistent with the π resonance picture since AB dimers do not have unpaired electrons, and therefore show no preference toward any specific sublattice position. There are of course exceptions, notably the values for adsorption onto $A(2)$ and $B(8)$ lattice sites, and these can be reasonably ascribed to the effect of surface relaxation. Indeed, relaxation energies per atom in "compact" clusters may considerably differ from the value of the single H atom, being always of the order of the binding energies themselves (~0.8 eV). Similar conclusions hold when adding a third H atom to the (magnetic) meta dimer $A(0)A(1)$: adsorption on B lattice sites is strongly favored (E_{bind}=1.2–1.9 eV) and produces doublet structures ($M=1\mu_B$), whereas H atoms bind to A lattice sites with an energy ~0.7–0.8 eV and produce highly magnetic structures ($M=3\mu_B$). Energy barriers to adsorption follow the same trend: preliminary calculations show that, with few exceptions, barriers to sticking a third H atom compare rather well with that for single H atom adsorption for the processes $AB \rightarrow A_2B$ and $A_2 \rightarrow A_3$ and may be considerably smaller for $A_2 \rightarrow A_2B$ ones.

In addition, again consistent with π resonance picture, we found that all the considered three-atom structures, with one or three unpaired electrons, show an alternation pattern in their spin-density maps. As an example, Fig. 8 reports the spin-density maps for an A_2B (left panel) and an A_3 (right panel) cluster. Analogous to Sec. III B we find that analysis of these spin-density maps gives insights to the adsorption properties of a fourth hydrogen atom. Table IV, for example, reports binding energies to form some four-atom clusters from the stable $A(0)B(2)B(8)$ one, the final total magnetization of the resulting structures and the values of the corresponding site-integrated magnetization before adsorption. The computed binding and barrier energies compare rather well with the dimer values, as can be seen in Figs. 6 and 7 where it is clear that the results fit well to the *same* linear trends obtained before. Few exceptions are for compact clusters where substrate relaxation does play some role. With such exceptions in mind, our results suggest that adsorption of hydrogen atoms on magnetic graphitic substrates (such as those obtained by adsorbing any odd number of H atoms), for a given final spin state, depends on the local spin density *only*.

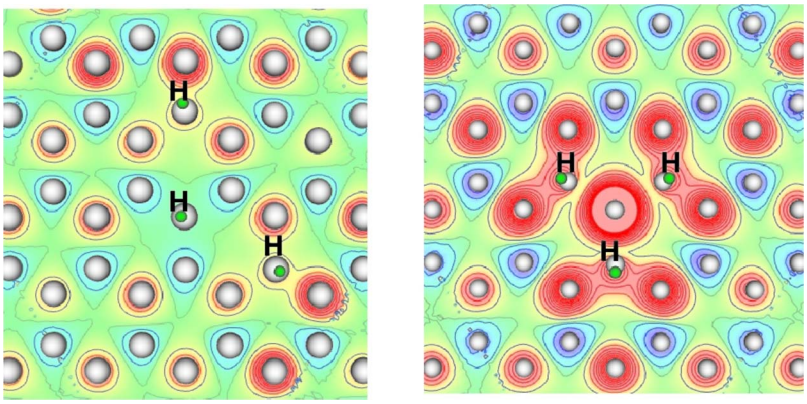

FIG. 8. (Color online) Spin density at 0.40 Å above the surface for two three-atom clusters. Contour map with red/blue lines for spin-up/spin-down excess, respectively. Left and right panels for A_2B and A_3 clusters, respectively.

IV. SUMMARY AND CONCLUSIONS

In this work we have presented results of extensive first-principles calculations of the adsorption properties of hydrogen atoms on graphite. A number of possible configurations involving one, two, three, and four atoms on the surface have been considered and barrier energies have been computed for some of them. We have found that adsorption of hydrogen atoms is strongly related to substrate electronic properties and used the chemical model of planar π conjugated systems to rationalize the data. The connection between this model and the valence theory of chemical bond on the one hand, and Hubbard models on the other hand, has been emphasized in Sec. III A and used at a qualitative level to rationalize our findings. In this way, one prominent feature of defective graphitic substrates, i.e., the possibility of forming ordered (microscopic) magnetic patterns, turns out to be related to the spin alternation typical of π resonant systems. We have also invariably found in the cases considered that Lieb's theorem for repulsive Hubbard models can be used to predict spin alignment in ground-state graphitic structures.

Adsorption of single H atoms has been known for some time to be an activated process, with an energy barrier to sticking (we find ~0.14 eV) high enough to prevent adsorption at ambient conditions. Adsorption of a second atom more favorably occurs on the $\sqrt{3}\times\sqrt{3}R30°$ sublattice where spin density localizes and may proceed without barrier if it occurs on the so-called para site. This preferential sticking has been recently suggested by experimental and theoretical observations by Hornekær *et al.*[38,39] We have extended the latter analysis by considering a large number of possible dimers and found that (i) binding (barrier) energies generally increase (decrease) linearly as a function of the site-integrated magnetization, and (ii) adsorption properties of the ortho site are slightly at variance with linear trends, thereby suggesting that substrate relaxation plays some role in this case.

When considering addition of a third atom we have found that the adsorption energetics of the incoming H atom is similar to that of the first one (i.e., a barrier ~0.15 eV high and a chemisorption well ~0.8 eV deep), unless we start with a "magnetic" dimer in which the two atoms are adsorbed in the same sublattice. (These structures, however, are kinetically and thermodynamically unfavored with respect to the unmagnetized *AB* configurations). This is in agreement with the chemical model, which predicts an "open-shell" configuration for A_2 dimers and a "closed-shell" one (with partial restoring of the π aromaticity) for *AB* ones. These results, therefore, suggest that preferential sticking due to barrierless adsorption is limited to formation of hydrogen pairs.

Finally, we have considered adsorption energetics in forming clusters of four atoms and regained the same picture obtained in forming pairs, namely, that adsorption is strongly biased toward the sublattice in which the spin density localizes. Actually, the resulting energetics fits well to the linear behavior with respect to the site-integrated magnetization already found for dimer formation. Such a linear relationship suggests that the energy needed to localize the unpaired electron on a given lattice site decreases linearly when increasing the site-integrated magnetization, at least in the range of values covered by this study. Interestingly, this behavior suggests that if we were able to tune the magnetization of the substrate we could *control* the adsorption dynamics of H atoms.

Overall our results, consistent with the π resonance picture, suggest that the *thermodynamically* and *kinetically* favored structures are those that minimize sublattice imbalance, i.e., those A_nB_m structures for which $n_I=|n-m|$ is minimum. The latter number n_I is also the number of midgap states in single-particle spectra which, according to the Hund-like rule provided by Lieb's theorem,[99] is directly related to the total spin of the system, $S=n_I/2$, which is therefore at minimum in the favored structures. Notice that however small the S value can be, this result does not preclude the existence of local magnetic structures, antiferromagnetically coupled to each other. The case of an *AB* dimer with two atoms very far from each other provides such an example.

ACKNOWLEDGMENTS

The authors thank the NOTUR consortium and the CILEA computing center for providing computational resources. S.C. acknowledges the University of Oslo for the hospitality during his stay.

[1] K. S. Novoselov, A. K. Geim, S. V. Morozov, D. Jiang, Y. Zhang, S. V. Dubonos, I. V. Gregorieva, and A. A. Firsov, Science **306**, 666 (2004).
[2] P. R. Wallace, Phys. Rev. **71**, 622 (1947).
[3] K. S. Novoselov, A. K. Geim, S. V. S. V. Morozov, D. Jiang, M. I. Katsnelson, I. V. Gregorieva, S. V. Dubonos, and A. A. Firsov, Nature (London) **438**, 197 (2005).
[4] Y. Zhang, Y.-W. Tan, H. L. Stormer, and P. Kim, Nature (London) **438**, 201 (2005).
[5] A. H. Castro Neto, F. Guinea, N. M. R. Peres, K. S. Novoselov, and A. K. Geim, Rev. Mod. Phys. **81**, 109 (2009).
[6] V. Meregalli and M. Parrinello, Appl. Phys. A: Mater. Sci. Process. **72**, 143 (2001).
[7] M. Mayer, V. Philipps, P. Wienhold, H. H. J. Seggern, and M. Rubel, J. Nucl. Mater. **290–293**, 381 (2001).
[8] L. Schlapbach and A. Züttel, Nature (London) **414**, 353 (2001).
[9] *The Molecular Astrophysics of Stars and Galaxies*, edited by T. W. Hartquist and D. A. Williams (Clarendon, Oxford, 1999).
[10] R. J. Gould and E. E. Salpeter, Astrophys. J. **138**, 393 (1963).
[11] D. Hollenbach and E. E. Salpeter, J. Chem. Phys. **53**, 79 (1970).
[12] D. Hollenbach and E. E. Salpeter, Astrophys. J. **163**, 155 (1971).
[13] J. Mayo Greenberg, Surf. Sci. **500**, 793 (2002).
[14] D. A. Williams and E. Herbst, Surf. Sci. **500**, 823 (2002).
[15] B. T. Draine, Annu. Rev. Astron. Astrophys. **41**, 241 (2003).
[16] L. Jeloaica and V. Sidis, Chem. Phys. Lett. **300**, 157 (1999).
[17] X. Sha and B. Jackson, Surf. Sci. **496**, 318 (2002).
[18] X. Sha, B. Jackson, and D. Lemoine, J. Chem. Phys. **116**, 7158 (2002).
[19] T. Zecho, A. Güttler, X. Sha, B. Jackson, and J. Küppers, J. Chem. Phys. **117**, 8486 (2002).
[20] X. Sha, B. Jackson, D. Lemoine, and B. Lepetit, J. Chem. Phys. **122**, 014709 (2005).
[21] S. Morisset, F. Aguillon, M. Sizun, and V. Sidis, J. Chem. Phys. **121**, 6493 (2004).
[22] A. Allouche, Y. Ferro, T. Angot, C. Thomas, and J.-M. Layet, J. Chem. Phys. **123**, 124701 (2005).
[23] S. Morisset, F. Aguillon, M. Sizun, and V. Sidis, J. Chem. Phys. **122**, 194702 (2005).
[24] R. Martinazzo and G. F. Tantardini, J. Phys. Chem. A **109**, 9379 (2005).
[25] N. Rougeau, D. Teillet-Billy, and V. Sidis, Chem. Phys. Lett. **431**, 135 (2006).

[26] A. Allouche, A. Jelea, F. Marinelli, and Y. Ferro, Phys. Scr., T **T124**, 91 (2006).
[27] J. Kerwin, X. Sha, and B. Jackson, J. Phys. Chem. B **110**, 18811 (2006).
[28] R. Martinazzo and G. F. Tantardini, J. Chem. Phys. **124**, 124702 (2006).
[29] R. Martinazzo and G. F. Tantardini, J. Chem. Phys. **124**, 124703 (2006).
[30] M. Bonfanti, R. Martinazzo, G. F. Tantardini, and A. Ponti, J. Phys. Chem. C **111**, 5825 (2007).
[31] H. Cuppen and L. Hornekær, J. Chem. Phys. **128**, 174707 (2008).
[32] Z. Medina and B. Jackson, J. Chem. Phys. **128**, 114704 (2008).
[33] Y. Ferro, D. Teillet-Billy, N. Rougeau, S. Morriset, and A. Allouche, Phys. Rev. B **78**, 085417 (2008).
[34] A. Güttler, T. Zecho, and J. Küppers, Chem. Phys. Lett. **395**, 171 (2004).
[35] T. Zecho, A. Güttler, and J. Küppers, Carbon **42**, 609 (2004).
[36] A. Güttler, T. Zecho, and J. Küppers, Surf. Sci. **570**, 218 (2004).
[37] A. Andree, M. Le Lay, T. Zecho, and J. Küppers, Chem. Phys. Lett. **425**, 99 (2006).
[38] L. Hornekaer, Z. Sljivancanin, W. Xu, R. Otero, E. Rauls, I. Stensgaard, E. Laegsgaard, B. Hammer, and F. Besenbacher, Phys. Rev. Lett. **96**, 156104 (2006).
[39] L. Hornekaer, E. Rauls, W. Xu, Z. Sljivancanin, R. Otero, I. Stensgaard, E. Laegsgaard, B. Hammer, and F. Besenbacher, Phys. Rev. Lett. **97**, 186102 (2006).
[40] S. Baouche, G. Gamborg, V. V. Petrunin, A. C. Luntz, A. Baurichter, and L. Hornekaer, J. Chem. Phys. **125**, 084712 (2006).
[41] S. C. Creighan, J. S. Perry, and S. D. Price, J. Chem. Phys. **124**, 114701 (2006).
[42] F. Islam, E. R. Latimer, and S. D. Price, J. Chem. Phys. **127**, 064701 (2007).
[43] L. Hornekær, W. Xu, R. Otero, T. Zecho, E. Laegsgaard, and F. Besenbacher, Chem. Phys. Lett. **446**, 237 (2007).
[44] V. M. Pereira, F. Guinea, J. M. B. Lopes dos Santos, N. M. R. Peres, and A. H. Castro Neto, Phys. Rev. Lett. **96**, 036801 (2006).
[45] O. V. Yazyev and L. Helm, Phys. Rev. B **75**, 125408 (2007).
[46] L. Pisani, B. Montanari, and N. M. Harrison, New J. Phys. **10**, 033002 (2008).
[47] V. M. Pereira, J. M. B. Lopes dos Santos, and A. H. Castro Neto, Phys. Rev. B **77**, 115109 (2008).
[48] J. J. Palacios, J. Fernandez-Rossier, and L. Brey, Phys. Rev. B **77**, 195428 (2008).
[49] O. V. Yazyev, Phys. Rev. Lett. **101**, 037203 (2008).
[50] M. Bonfanti, R. Martinazzo, G. F. Tantardini, and A. Ponti (unpublished).
[51] G. Kresse and J. Hafner, Phys. Rev. B **49**, 14251 (1994).
[52] G. Kresse and J. Hafner, Phys. Rev. B **47**, 558 (1993).
[53] G. Kresse and J. Furthmüller, Comput. Mater. Sci. **6**, 15 (1996).
[54] G. Kresse and J. Furthmuller, Phys. Rev. B **54**, 11169 (1996).
[55] P. E. Blochl, Phys. Rev. B **50**, 17953 (1994).
[56] G. Kresse and D. Joubert, Phys. Rev. B **59**, 1758 (1999).
[57] J. P. Perdew, K. Burke, and M. Ernzerhof, Phys. Rev. Lett. **77**, 3865 (1996).
[58] J. P. Perdew, K. Burke, and M. Ernzerhof, Phys. Rev. Lett. **78**, 1396 (1997).
[59] P. E. Blochl, O. Jepsen, and O. K. Andersen, Phys. Rev. B **49**, 16223 (1994).
[60] M. Hasegawa and K. Nishidate, Phys. Rev. B **70**, 205431 (2004).
[61] H. Rydberg, N. Jacobsen, P. Hyldgaard, S. I. Simak, B. I. Lundqvist, and D. C. Langreth, Surf. Sci. **532–535**, 606 (2003).
[62] J. Kerwin and B. Jackson, J. Chem. Phys. **128**, 084702 (2008).
[63] Y. Ferro, F. Marinelli, and A. Allouche, Chem. Phys. Lett. **368**, 609 (2003).
[64] E. J. Duplock, M. Scheffler, and P. J. D. Lindan, Phys. Rev. Lett. **92**, 225502 (2004).
[65] T. Roman, W. A. Diño, H. Nakanishi, H. Kasai, T. Sugimoto, and K. Tange, Carbon **45**, 218 (2007).
[66] L. Chen, A. C. Cooper, G. P. Pez, and H. Cheng, J. Phys. Chem. C **111**, 18995 (2007).
[67] P. O. Lehtinen, A. S. Foster, Y. Ma, A. V. Krasheninnikov, and R. M. Nieminen, Phys. Rev. Lett. **93**, 187202 (2004).
[68] D. W. Boukhvalov, M. I. Katsnelson, and A. I. Lichtenstein, Phys. Rev. B **77**, 035427 (2008).
[69] M. Inui, S. A. Trugman, and E. Abrahams, Phys. Rev. B **49**, 3190 (1994).
[70] H. A. Mizes and J. S. Foster, Science **244**, 559 (1989).
[71] P. Ruffieux, O. Groning, P. Schwaller, L. Schlapbach, and P. Groning, Phys. Rev. Lett. **84**, 4910 (2000).
[72] K. Kusakabe and M. Maruyama, Phys. Rev. B **67**, 092406 (2003).
[73] D. Jiang, B. G. Sumpter, and S. Dai, J. Chem. Phys. **127**, 124703 (2007).
[74] O. V. Yazyev, W. L. Wang, S. Meng, and E. Kaxiras, Nano Lett. **8**, 766 (2008).
[75] O. V. Yazyev and M. I. Katsnelson, Phys. Rev. Lett. **100**, 047209 (2008).
[76] L. Pauling and E. B. Wilson, *Introduction to Quantum Mechanics With Applications to Chemistry* (McGraw-Hill, New York, 1935).
[77] W. Heitler and F. London, Z. Phys. **44**, 455 (1927).
[78] G. F. Tantardini, M. Raimondi, and M. Simonetta, Int. J. Quantum Chem. **7**, 893 (1973).
[79] M. Raimondi, M. Simonetta, and G. F. Tantardini, Comput. Phys. Rep. **2**, 171 (1985).
[80] G. Rumer, Nachr. Ges. Wis. Gott., Math-Physik Klasse (1932) 377.
[81] J. Gerratt, Adv. At. Mol. Phys. **7**, 141 (1971).
[82] D. L. Cooper, J. Gerratt, and M. Raimondi, Chem. Rev. (Washington, D.C.) **91**, 929 (1991).
[83] D. L. Cooper, *Valence Bond Theory*, Theoretical and Computational Chemistry Vol. 10 (Elsevier, Amsterdam, 2002).
[84] J. Li and R. McWeeny, Int. J. Quantum Chem. **89**, 208 (2002).
[85] G. F. Tantardini, M. Raimondi, and M. Simonetta, J. Am. Chem. Soc. **99**, 2913 (1977).
[86] D. L. Copper, J. Gerratt, and M. Raimondi, Nature (London) **323**, 699 (1986).
[87] D. L. Cooper, J. Gerratt, and M. Raimondi, in *Ab Initio Methods in Quantum Chemistry II*, edited by K. P. Lawley (Wiley, New York, 1987).
[88] J. Hubbard, Proc. R. Soc. London, Ser. A **276**, 238 (1963).
[89] J. Wu, T. G. Schmalz, and D. J. Klein, J. Chem. Phys. **117**, 9977 (2002).
[90] J. Wu, T. G. Schmalz, and D. J. Klein, J. Chem. Phys. **119**, 11011 (2003).
[91] R. Pariser and R. G. Parr, J. Chem. Phys. **21**, 466 (1953).
[92] R. Pariser and R. G. Parr, J. Chem. Phys. **21**, 767 (1953).
[93] J. A. Pople, Trans. Faraday Soc. **49**, 1375 (1953).
[94] A. Cresti, N. Nemec, B. Biel, G. Niebler, F. Triozon, G. Cuniberti, and S. Roche, Nano Res **1**, 361 (2008).
[95] J. Fernandez-Rossier, Phys. Rev. B **77**, 075430 (2008).
[96] J. Li, B. Duke, and R. McWeeny, VB Version 2.0, SciNet Technologies, San Diego, CA, 2007.
[97] M. W. Schmidt, K. K. Baldridge, J. A. Boatz, S. T. Elbert, M. S. Gordon, J. H. Jensen, S. Koseki, N. Matsunaga, K. A. Nguyen, S. J. Su, T. L. Windus, M. Dupuis, and J. A. Montgomery, J. Comput. Chem. **14**, 1347 (1993).
[98] R. McWeeny, Adv. Quantum Chem. **31**, 15 (1998).
[99] E. H. Lieb, Phys. Rev. Lett. **62**, 1201 (1989).